chemosensors

Article

Insight into Reduction Process of Diquat on Silver and Copper Electrodes Studied Using SERS

María Rosa López-Ramírez [1,*], Lucas Olivares-Fernández [1] and Santiago Sanchez-Cortes [2]

[1] Department of Physical Chemistry, Faculty of Science, University of Málaga, 29071 Málaga, Spain; olivares1416@uma.es
[2] Instituto de Estructura de la Materia, CSIC, Serrano, 121, 28006 Madrid, Spain; s.sanchez.cortes@csic.es
* Correspondence: mrlopez@uma.es

Abstract: A surface-enhanced Raman scattering (SERS) study of diquat (DQ) on silver and copper electrodes is presented in this work in order to complete previous studies on the SERS of DQ on metal nanoparticles. We supported the experimental results with theoretical calculations of different species of DQ, analyzing the most important molecular differences and their corresponding Raman spectra. DQ SERS spectra on Ag and Cu electrodes were obtained at different excitation wavelengths. An analysis of the SERS spectra revealed that at more positive electrode potentials, the interaction of DQ with the metal formed a charge-transfer complex via the chloride anion previously adsorbed on the surface; additionally, at more negative potentials, other species of diquat, such as DQ^{2+}, could be directly adsorbed on the metal's surface. Finally, we detected new SERS bands corresponding to DQ at negative electrode potentials that were sensitive to the excitation wavelength, suggesting that lateral interactions between radical cation species on the electrode surface lead to intramolecular dimerization and a possible multilayer of the adsorbate.

Keywords: diquat; SERS; silver electrode; copper electrode; DFT calculations

check for updates

Received: 19 November 2024
Revised: 14 January 2025
Accepted: 21 January 2025
Published: 27 January 2025

Citation: López-Ramírez, M.R.; Olivares-Fernández, L.; Sanchez-Cortes, S. Insight into Reduction Process of Diquat on Silver and Copper Electrodes Studied Using SERS. *Chemosensors* **2025**, *13*, 39. https://doi.org/10.3390/chemosensors13020039

Copyright: © 2025 by the authors. Licensee MDPI, Basel, Switzerland. This article is an open access article distributed under the terms and conditions of the Creative Commons Attribution (CC BY) license (https://creativecommons.org/licenses/by/4.0/).

1. Introduction

Surface-enhanced Raman spectroscopy (SERS) is a key tool in surface analysis, attending to two primary purposes: firstly, to explore the origin and mechanisms behind the Raman enhancement and the magnitude of the SERS enhancement factor, and secondly, to directly evaluate the SERS intensity of a target molecule for analytical applications. Regarding the first aspect, the magnitude of the SERS enhancement is crucial for understanding both the origin of the SERS signal and its enhancement mechanisms. The primary contribution to the SERS enhancement comes from the intense electromagnetic field generated by the localized surface plasmon resonances of nanometric particles or clusters [1,2]. Furthermore, the SERS technique proves to be highly effective in studying charge-transfer reactions occurring between a metal surface and an adsorbed molecule. One of the key advantages of SERS in this context is its ability to provide a detailed vibrational spectrum of the molecules adsorbed onto the surface. This spectrum not only reveals information about their molecular vibrations but also offers valuable insights into the orientation and conformation of the adsorbed species. By analyzing the shifts and intensities of specific vibrational bands, researchers can infer how the molecules interact with the metal surface, including their alignment relative to the surface and any conformational changes induced by the adsorption process. This makes SERS a powerful tool for understanding the complex dynamics of surface interactions, including charge-transfer processes.

Additionally, SERS electrochemistry (EC-SERS) remains a highly active area of research due to its unique ability to control and manipulate surface potential. This capability allows for precise control over adsorption and desorption processes and charge-transfer phenomena, as well as the investigation of molecular orientation on a surface. In this type of electrochemical experiment, the electronic charge transfer between the molecule and the metal, whether in the opposite direction or not, can be followed by observing the shift in the potential, at which maximum intensity occurs, relative to the photon energy of the incident light [3–7]. While the electromagnetic mechanism (EM) is widely recognized as the general enhancement mechanism operating in SERS, it cannot fully explain the strong dependence of these spectra on the electrical potential at the interface. Thus, the complementary charge-transfer (CT) mechanism, which is highly dependent on the nature of both the metal and the adsorbate, as well as the specific experimental conditions, allows us to correlate our SERS results with molecular changes.

Once the main experimental technique of this work has been introduced, we want to focus on a group of compounds that are very relevant today that increasingly constitutes a very necessary field of study. We are referring to the field of herbicides, and within this topic, probably the best-known herbicides available are methyl viologens (as the dichloride salt) and its other dibromide derivative, diquat (N,N′-ethylene-2,2′-bipyridynium, DQ). This herbicide and plant growth regulator is non-selective and chemically related to paraquat. It is commonly used in agriculture and can cause moderate liver and kidney toxicity in mammals, including humans [8–10]. Herbicidal activity appears to depend, in part, on the ease of the photolytic one-electron reduction of MV^{2+} or DQ^{2+} to form the stable but air-sensitive radical $MV^{+\bullet}$ or $DQ^{+\bullet}$, respectively. DQ belongs to the chemical family of viologens, which are dication species with interesting properties related to their redox chemistry, electron-poor nature, and possibility to form charge-transfer (CT) complexes [11]. Despite the clear relevance of this molecule in the aforementioned areas, it is surprising that a comprehensive vibrational assignment remains absent from the scientific literature. The only related studies include a brief report on the infrared spectrum of DQ in its dibromide form [12] and a more extensive investigation of the resonance Raman spectrum of both DQ and its radical cation [13]. More recently, we published a study on the Raman and SERS spectra of DQ on Ag nanoparticles [14], which opened a series of very interesting questions that we would like to try to answer in the present work. In this study, we present the first SERS investigation of DQ adsorbed on metal electrodes, examining the remarkable sensitivity of its key structural bands to molecular changes induced by both chemical reduction and the adsorption of DQ onto a metal surface. Notably, we observed clear changes upon its adsorption on Ag nanoparticles, such as an increase in molecular coplanarity. We concluded in our previous study [14] that DQ adopts a similar structure to the radical cation ($DQ^{+\bullet}$) species to better approach the metal surface, assisted by halide ions previously adsorbed onto the surface. The particular behavior of viologens, which are able to interact with surfaces, gives rise to an exciting field of study by combining the electromagnetic properties of metals and the electrochemical properties of viologens. Therefore, surface-enhanced vibrational techniques for DQ adsorbed on metallic surfaces could be very interesting for the trace detection of herbicides in the environment and for advancing our understanding of the electrochemistry of these compounds. Viologens were originally studied as redox indicators in biological research, and their significance persists today due to their possession of some of the most cathodic redox potentials of any organic system, with a notable degree of reversibility. They are also the parent compounds of the "paraquat" family, one of the new classes of herbicides discovered in recent years [15].

In relation to our investigation, there are few publications on the EC-SERS of DQ. However, we find it relevant to highlight other studies that explore the contribution of the

charge-transfer (CT) mechanism to the overall SERS enhancement, such as research on 2,2′-bipyridine (bpy) adsorbed on silver surfaces and the formation of Ag-bpy complexes [16], as well as the development of an electrochemical SERS sensor for the point-of-care testing of paraquat and diquat [17]. The innovative aspect of our EC-SERS study on DQ lies in the comparative analysis of this adsorbate's interaction with both silver (Ag) and copper (Cu) electrodes. Additionally, we provide a comprehensive study of the redox species of DQ on these metal electrodes, complemented by DFT calculations, to identify the interfacial species formed during adsorption. The use of Cu as an SERS substrate is relatively uncommon due to two main challenges: its tendency to oxidize, which weakens plasmon resonance, and the limited availability of reported stable nanostructures [18]. Despite these challenges, we successfully obtained and analyzed SERS spectra of DQ on Cu electrodes, expanding the understanding of Cu's potential as an SERS substrate.

2. Materials and Methods

2.1. Theoretical Calculations

The theoretical calculations were performed by using the "Picasso" computing machine, with the Gaussian 09 software product (USA) performing the optimization of the ground-state geometries and generating the theoretical spectrum of different DQ species. The density functional theory (DFT) with the B3LYP level of theory and the 6-31+G* and LanL2DZ were applied as the basis set for DQ species and DQ complexes, respectively [19]. The theoretical UV-Vis spectra of the DQ species and its metal complexes were calculated using the time-dependent (TD)-DFT method with the 6-31+G* and LanL2DZ basis set, respectively. The visualization of theoretical Raman, UV-Vis spectra and optimized molecular structures were carried out by using GaussView 5.0 software (USA). Raman spectra were corrected by a scaling factor of 0.98. Data representation and interpretation were performed by using OriginPro2023 software (USA). In some spectra, baseline corrections were necessary.

2.2. Materials and Instrumentation

$DQBr_2$ was acquired from Supelco with a purity of 99% w/w. Stock solutions of the dication were prepared in water. All the reagents employed were of analytical grade and purchased from Sigma-Aldrich (Germany). The aqueous solutions were prepared by using Milli-Q deionized water at 18 MΩ cm^{-1}.

A series of SERS measurements were measured in the electrochemical cell with 0.1 M KCl electrolyte and different concentration solutions of the studied compound. The SERS spectra obtained at 514.5, 632.8 and 785 nm were measured with a Renishaw InVia Qontor spectrometer (UK) and a macro system objective. The laser power at the sample was 2 mW and the spectral resolution was 4 cm^{-1}. The confocal microscope was equipped with a macro lens of f = 30 mm that we needed to analyze the working electrode on our electrochemical cell. In the case of the Cu electrode, it could not be used for plasmonic applications below ∼600 nm due to interfering interband transitions, and spectra were only acquired at 632.8 nm and 785 nm.

2.3. Electrode Preparation for SERS Study

An electrochemical cell 600 E, Ventacon (Southampton, UK) equipped with a three-electrode system, a reference KCl-saturated Ag/AgCl electrode, an auxiliary platinum wire electrode, and a working Ag or Cu electrode, was used for the SERS measurements. The preparation of the working electrode involved both mechanical cleaning and electrochemical activation. First, the electrode surface was carefully cleaned using 0.30 μm and 0.05 μm of Buehler Polishing Alumina MicroPolish powder (USA). For activation, the Ag

electrode was treated in a 0.1 M KCl solution, applying a potential of −0.5 V with a scan rate of 0.1 V/s. Electrochemical roughening was then performed by applying ten cycles of 2 s pulses at +0.6 V. For the Cu electrode, the activation involved applying a potential of −0.5 V with a scan rate of 0.1 V/s, followed by electrochemical roughening using ten cycles of 2 s pulses at +0.4 V. A VersaStat II potentiostat (Perkin-Elmer Instruments, Springfield, IL, USA) was used to control the electric potentials.

3. Results

3.1. Theoretical and Experimental Raman Spectra of Diquat

The organic molecule diquat (DQ) is a dication formed by the addition of an ethylene bridge between the nitrogen atoms of 2,2′-bipyridine, and its dibromide salt is the most commercial herbicide and stable compound. The herbicidal activity of DQ depends on the formation of a radical cation through one electron reduction, reorganizing the electronic molecular structure and consequently changing the molecular parameters. The information from DFT calculations about all the reduction species of DQ is very useful to understand the adsorption process on a metallic electrode. For this reason, in Table 1, the DFT and TD-DFT calculations of different species of DQ at the B3LYP/6-31+G* level of theory are shown, and their theoretical Raman spectra are represented in Figure 1. From Table 1, we have to highlight that the reduction of DQ^{2+} > $DQ^{+\bullet}$ > DQ^{0} gives rise to a decrease in the dihedral angle α (HC-C-C-CH) from 22.60° to only 4.76° and in the inter-ring C-C distance from 1.48 Å to 1.38 Å due to an increase in the molecular coplanarity. These structural changes affect other molecular properties like the UV-vis spectra. As we can observe, Table 1 also shows the corresponding UV-vis plot for the first excited state from TD-DFT calculations that are used to simulate the UV spectra and to determine the MOs involved in each transition [20]. We can observe that an increase in the coplanarity ($DQ^{+\bullet}$ and DQ^{0}) induces the red-shift of theoretical UV-vis to near-infrared and visible wavelengths, respectively. Furthermore, a general decrease in the oscillator strength in the spectra is observed.

The theoretical Raman spectra of these species were calculated and compared with the experimental Raman spectra of 0.5 M solution and the solid state of DQ^{2+} at several wavelengths. Figure 1 shows both the Raman experimental spectra recorded at 632.8 nm together with the calculated ones. The Raman spectra of DQ in solid and aqueous solution are also measured at 514.5 nm and 785 nm, but there are no relevant differences between them (see Figure S1, Supplementary Materials). This fact is explained on the basis of the UV-vis absorption spectrum of DQ^{2+}, the maxima of which are in the UV region (Table 1) and the absence of molecular resonance at these excitation wavelengths.

The theoretical Raman spectrum of DQ^{2+} (Figure 1A(c)) fits very well with the experimental Raman spectrum of the solution, even at the absolute intensity of the most important bands. The proposed assignment of this molecule in solution and in a solid state is shown in Table 2 by using the DFT calculations as the orientation. Three major bands at 1612, 1577 and 1327 cm^{-1} characterized the Raman spectrum. The bands at 1612 and 1577 cm^{-1} were attributed to totally symmetric ring stretching vibrations based on comparisons with similar assignments made for methyl pyridine chloride, biphenyl, and paraquat dichloride [21–23]. The band at 1327 cm^{-1} is assigned to a totally symmetric inter-ring stretching vibration, which is sensitive to rotation around the C–C inter-ring bond. This band is particularly important as it is responsive to changes associated with the possible delocalization of π-electron density within the rings. Due to the connecting ethylene chain between the two pyridine rings, the rotation is not allowed. Consequently, the dication in solution keeps the same structure rather than attaining the structure found in the solid state, and only a slight upshift of the bands corresponding to the totally symmetric modes is observed in the Raman spectrum of the aqueous solution of DQ^{2+} (Figure 1A(a)).

Table 1. DFT and TD-DFT calculations of different species of DQ^{2+} at the B3LYP/6-31+G* level of theory. UV-vis plots for the first excited state from TD-DFT calculations.

Dication: DQ^{2+}	Radical Cation: $DQ^{\bullet+}$	Neutral: DQ^{0}
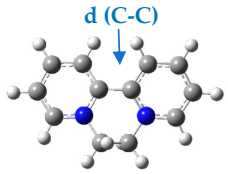	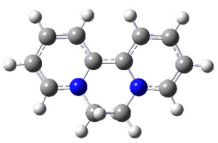	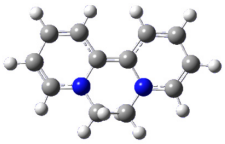
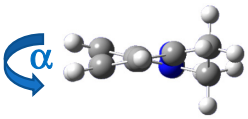	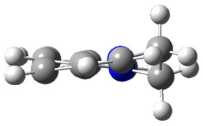	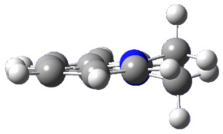
d (C-C) = 1.48 Å	d (C-C) = 1.43 Å	d (C-C) = 1.38 Å
α = 22.60°	α = 14.32°	α = 4.76°
E_{min} (a.u.) = −573.44010	E_{min} (a.u.) = −573.78443	E_{min} (a.u.) = −573.96443
Charge = 2, singlet	Charge = 1, doublet	Charge = 0, singlet
E_{HOMO} (Hartree) = −0.56570 E_{LUMO} (Hartree) = −0.39830 $Energy_{L-H}$ gap (eV) = 4.56	E_{HOMO} (Hartree) = −0.29055 E_{LUMO} (Hartree) = −0.19411 $Energy_{L-H}$ gap (eV) = 2.62	E_{HOMO} (Hartree) = −0.12846 E_{LUMO} (Hartree) = −0.02801 $Energy_{L-H}$ gap (eV) = 2.73
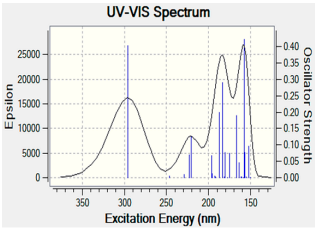	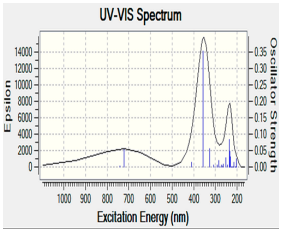	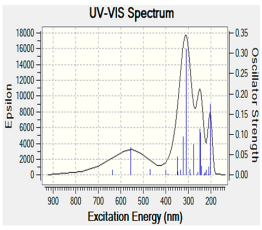
λ = 295 nm, 157 nm	λ = 720 nm, 355 nm	λ = 556 nm, 310 nm

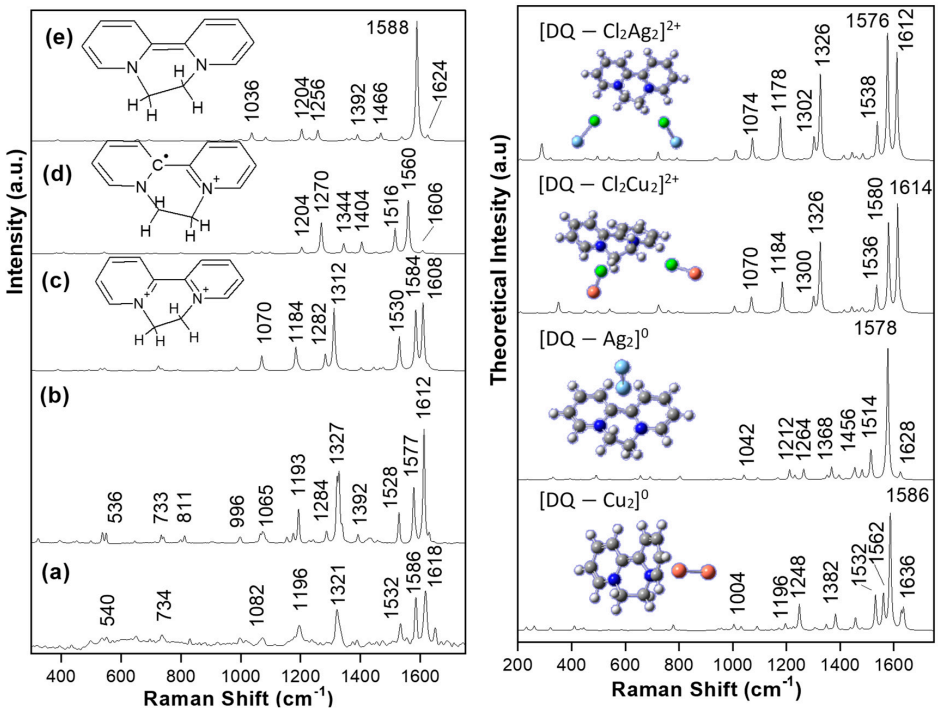

(**A**) (**B**)

Figure 1. (**A**) Raman spectra of 0.5 M solution of DQ^{2+} (**a**) and in the solid state (**b**) recorded at 632.8 nm. Theoretical Raman spectra of different species: DQ^{2+} (**c**), $DQ^{\bullet+}$ (**d**) and DQ^{0} (**e**). (**B**) Theoretical Raman spectra of copper and silver complexes of DQ^{2+}.

Table 2. Experimental and calculated vibrational frequencies (cm^{-1}) of DQ^{2+}.

ν_{calc} [a]	ν_{Raman} [b]		Assignment [c]
B3LYP/6-31+G*	**Solid**	**Aqueous 1M**	
390 vw	394 vw		δ_{ring}
530 vw	536 vw	540 vw	γ_{ring}
726 vw	733 vw	734 vw	δ_{ring}
986 vw	996 vw		$\nu(H_2C\text{-}CH_2)$
1068 w	1065 w	1082 w	$r(CH_2) + \delta_{ring}$
	1156 vw		$\delta(CH) + \nu_{ring}$
	1175 vw		$\delta(CH) + \nu_{ring}$
1184 w	1193 w	1196 w	$\delta(CH) + \nu(CH_2\text{-}N)$
1282 w	1284 vw	1290 vw	$\nu(C\text{-}C)_{inter\text{-}ring}$
1310 s	1327 s	1321 s	$\nu(C\text{-}C)_{inter\text{-}ring}$
1440 vw	1433 vw	1440 vw	$w(CH_2)$
1460 vw	1458 vw	1472 vw	$\delta(CH_2)$
1530 m	1528 w	1532 w	$\nu_{ring} + \nu(C{=}N)$
1584 s	1577 m	1586 m	$\nu_{ring} + \nu(C{=}N)$
1610 s	1612 s	1618 s	8a; $\nu_{ring} + \nu(C{=}N)$

[a] Calculated wavenumber at B3LYP/6-31+G* level of theory of DQ^{2+}. [b] Raman frequencies at 632.8 nm. [c] Abbreviations: w—weak; vw—very weak; m—medium; s—strong; vs—very strong; ν—stretching; δ—bending; γ—out of plane; r—rocking.

The DQ^{2+} cation is found to be very stable in solution and it does not degrade with time, leading to its reduced species. As a result, its Raman spectra in the solid state and in solution are also very reproducible with time. We can appreciate in Figure 1A that due to the decrease in the inter-ring angle in the reduced species and other molecular changes, the corresponding vibrational spectra of the radical cation and neutral species are modified, especially the inter-ring vibrational modes around 1300 cm^{-1} and the ν(C=N) around 1600 cm^{-1}. These vibrational shifts are very important in understanding the adsorption of DQ on metal surfaces and detecting the possible formation of new adsorbates.

3.2. SERS Spectra of Diquat on Silver and Copper Electrodes

In previous SERS studies of DQ [14] on silver colloids, we observed structural changes when it was adsorbed onto silver nanoparticles, consisting of a partial sp^2 to sp^3 transition, giving rise to an increase in molecular coplanarity. We concluded that the strong electron-accepting nature of the DQ dication enabled it to interact with silver, forming a charge-transfer complex through the anion adsorbed on the surface. Another notable finding from this study was the analysis of DQ SERS at varying viologen concentrations, which showed that at high concentrations, the adsorbate formed a multilayer. Additionally, the corresponding SERS spectra were found to be sensitive to the excitation wavelength.

The present work tries to go further in the investigation of the adsorption process of DQ by using metal electrodes as SERS substrates, with the main aim of comparing the behavior of this adsorbate by modifying the interfacial potential, the electrode metal or the excitation wavelengths. The current literature on the SERS of DQ on metal electrodes is very limited and even more so if we try to find vibrational studies centered on the adsorption process of DQ on metal substrates because most of the applications are focused on the detection of this herbicide by different methods such as the development of biosensors [17,24,25]. Due to the poorer localized surface plasmon resonances of Cu, its electromagnetic enhancement is weaker than that of Ag and Au. The SERS enhancement factor obtained for simple copper substrates was reported to be 10^3–10^7 [26,27], being lower than that of silver (10^6–10^{14}) and gold (10^4–10^9) [28,29]. The metal electrode substrates produce more compact nanoparticles, which favor the plasmonic properties of Cu, and the SERS spectra reached in this work is quite acceptable.

Figures 2 and 3 show SERS spectra of DQ 10^{-5} M on copper and silver electrodes recorded at 632.8 nm and 785 nm, respectively. At both wavelengths, the SERS spectra at more positive potentials are quite similar to those obtained in metal colloids in previous studies [14]; that is, the most intense band appears at 1578 cm^{-1} ($\nu_{ring} + \nu(C{=}N)$), and bands

around 1318, 1260, 1176, 1060 and 733 cm^{-1} relating to ν(C-C) $_{inter\text{-}ring}$ and δ(CH) are also present. The position of these bands changes with the nature of the metal, especially when the SERS spectra are registered at more negative potentials. If we compare with the Raman spectrum of the DQ in solution (Figure 1A(a)), important differences are detected like a strong intensity decrease in the 1618 cm^{-1} band, together with a downshift to 1608 cm^{-1}. Moreover, it is noted that there is an intensification of the band at 1586 cm^{-1}, which undergoes a shift downward to around 1580 cm^{-1}.

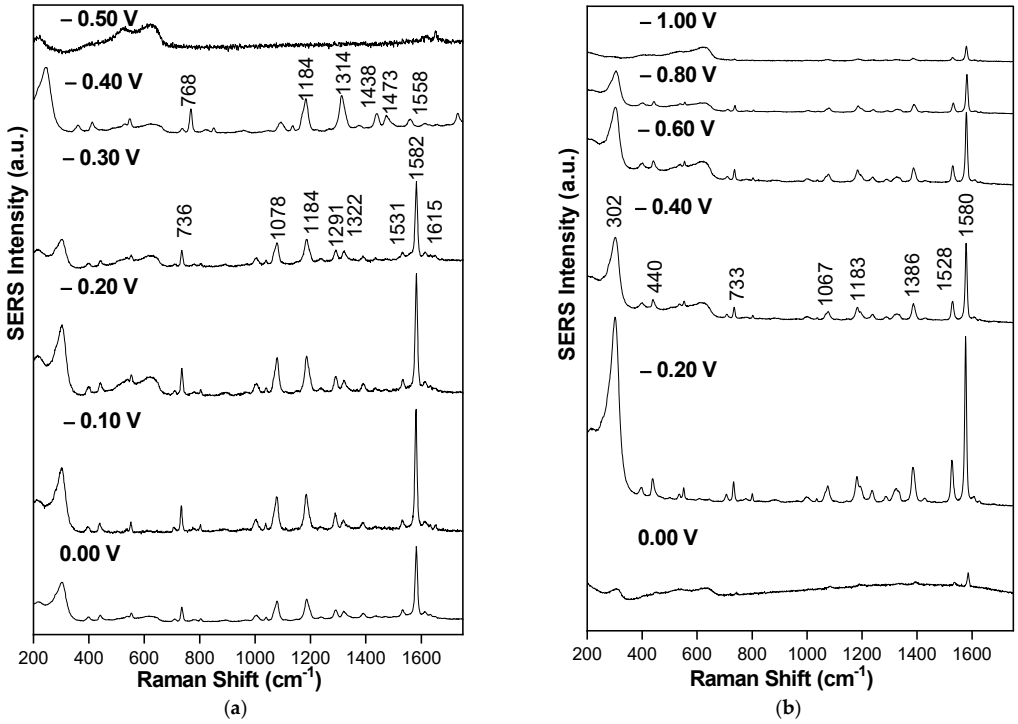

Figure 2. SERS spectra of DQ^{2+} 10^{-5} M on copper electrode recorded at (**a**) 632.8 nm, (**b**) 785 nm.

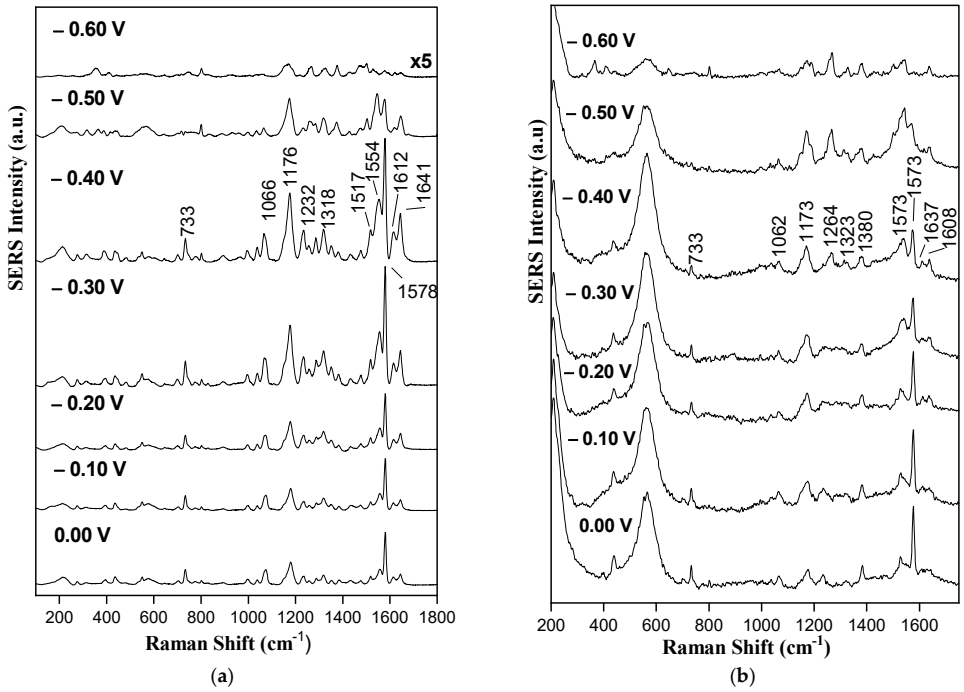

Figure 3. SERS spectra of DQ^{2+} 10^{-5} M on silver electrode recorded at (**a**) 632.8 nm, (**b**) 785 nm.

DQ's behavior observed in this study closely resembles previous findings involving another different substrate such as silver colloid [14]. According to these earlier observations, we confirm that the enhancement of the relevant band can be attributed to the formation of a strong ionic pair between the cation and the anion, in this case, chloride ions (Cl^-) from the electrolyte solution. These chloride ions are known to adsorb onto the metal surface, a phenomenon that has also been observed with other cationic species [30–33]. The interaction between the nitrogen atoms (N) of DQ and the chloride ions appears to be so strong that it leads to a charge transfer between the halide and DQ, similar to what has been investigated on other viologen species [34]. This charge transfer interaction induces a significant weakening of the CN^+ bond, promoting a partial transition from an sp^2 to an sp^3 hybridization state. This transition accounts for the noticeable spectral changes observed in the corresponding region, highlighting the impact of this CT interaction on the molecular structure of DQ.

The bands recorded at 1322, 1291 and 1184 cm^{-1} are markedly intensified in the SERS of DQ on the Cu or Ag electrode at more positive potentials, which, in principle, is consistent with previously observed data, and they are related to vibrations of the C–N bonds. In this sense, it is important to mention the very low intensity of the band at 1618 cm^{-1} in all the cases, which is assigned in the Raman spectrum of the DQ solution to 8a, the ν_{ring} vibrational mode of the DQ^{2+} species, which indicates that the amount of diquat adsorbed without interaction with the anion is rather poor. In order to confirm previous conclusions extracted from the observation of the experimental results, we calculate the theoretical Raman spectra of several metal complexes of DQ^{2+} (see Figure 1B). In all the cases, we start with DQ^{2+}, $DQ^{+\bullet}$ and DQ^0 species and different charges on the metal cluster, but we are able to optimize only the DQ^{2+} complexes: DQ-Ag_2, DQ-Cl_2Cu_2 and DQ-Cl_2Ag_2 represented in Figure 1B. The stable DQ-Ag_2 complex is obtained at the negative silver charge, but the dication metal complexes, DQ-Cl_2Cu_2 and DQ-Cl_2Ag_2, are stable at the positive metal charge, considering, in the case of copper, only the mono positive copper (Cu^+). Based on these primary calculations, we concluded that the possibility of adsorption through the interaction with the anions is possible at more positive potentials, and in addition, at negative potentials, the formation of direct DQ-Ag_2 is also possible. The formation of the silver complex at negative potentials also changes the inter-ring dihedral angle from 22.60° (DQ^{2+}) to 5.42° (DQ-Ag_2) and 13.35° (DQ-Cu_2), and there is a reduction in the C-C inter-ring bond distance in both complexes. These geometrical changes simulate the situation during the adsorption, and we can observe that the theoretical Raman spectra of both silver and copper complexes are quite similar to those of the radical cation shown in Figure 1A(d). Consequently, we suggest that the SERS spectra at more negative potentials have contributions from different species. In fact, one can identify the radical cation formed near the metal surface as well as the metal complexes of the dication species that make possible the interaction of the direct complex without the ion chloride as an intermediary in the adsorption process. In general, the SERS spectra of DQ at more positive potentials are quite similar on Cu and Ag electrodes. However, at potentials more negative than −0.30 V, the SERS spectra of DQ on the Ag electrode change, while in the SERS spectra on the Cu electrode, no important changes are detected. The number, position and intensity of the new SERS bands at −0.40 V on the Ag electrode do not correlate with our results from the normal Raman spectra of diquat solution or in a solid state (Table 2). This fact suggests the generation of new species at these negative potentials. We propose that DQ^{2+} give rise to $DQ^{+\bullet}$ on the electrode surface by accepting one electron in a fast reaction. Moreover, the latter species are strongly adsorbed on the silver surface, replacing the dication [35]. Therefore, once the radical cation is produced, we are able to observe different SERS spectra at −0.40 V (Figure 3a,b).

The electrochemical behavior of DQ on the Cu electrode exhibits noticeable changes at −0.40 V when excited at 632.8 nm. In contrast, no spectral changes are observed at 785 nm,

although a decrease in the absolute Raman intensities is detected at negative potentials in the latter case. The voltammograms of the SERS experiment of DQ on Ag and Cu electrodes are shown in Figure 4. The first adsorption peak was seen, in both cases, near −0.40 V, which indicates the reduction process of the first one-electron transfer, leading to a coverage of silver or copper electrodes by $DQ^{+\bullet}$. The latter radical cation is probably adsorbed, adopting a flat orientation as other authors [35] have also concluded. The further reduction step giving rise to the formation of DQ^0 is greatly influenced by the experimental conditions through the comproportionation reaction [36]: $DQ^{2+} + DQ^0 \rightarrow 2DQ^{+\bullet}$. In most of the SERS experiments, we are not able to acquire SERS spectra at an electrode potential more negative than −0.60 V, so we believe that it is not very likely that this species is present as an adsorbate.

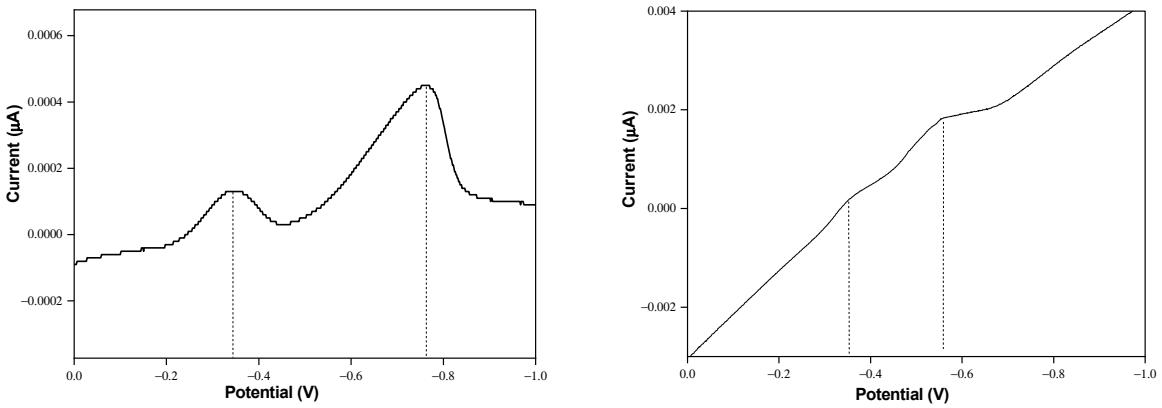

Figure 4. Voltammograms of DQ^{2+} 10^{-5} M (0.1 M KCl) recorded on (**a**) copper electrode and (**b**) silver electrode. Scan rate 100 mV s^{-1}.

We believe that the reduction of diquat on the electrode surface occurs in the same way as it does in some processes, which give rise to adsorption–nucleation peaks. For example, heptyl viologen on a polycrystalline silver electrode forms a film of radical cations that adsorb chloride salt and are deposited onto the electrode surface [30]. Additionally, as we have proposed in previous works [14], at a relative low concentration such as 10^{-5} M, a full surface coverage by DQ is expected, taking into account the size of the adsorbate and the overall exposed metal surface. At concentrations above this level, DQ adsorbs onto the first layer, forming multilayers. This multilayer formation is enhanced at more negative potentials on the metal electrode. The SERS spectra of DQ 10^{-3} M on the Cu electrode are shown in Figure S2 (Supplementary Materials), and we observe an increase in the signal-to-noise background from an electrode potential of −0.60 V, probably due to the formation of these multilayers. The same happens in the SERS of DQ on the silver electrode when we excite it by using the 514.5 nm laser line because of a resonance Raman effect of the secondary products (Figure S3, Supplementary Materials) such as the radical cation and the dimer, which has an absorption band similar to the former [34]. Figure 5 shows the proposed interaction of the DQ monomer and dimer at more negative potentials. Based on our experimental results, we suggest that at more negative electrode potentials, anion desorption is favored, leading to a noticeable decrease in the Ag–Cl stretching band around 302 cm^{-1}. Under these conditions, other species different from radical cations can approach the metal surface, contributing to the overall SERS signal and giving rise to the formation of multilayers that may contain various species.

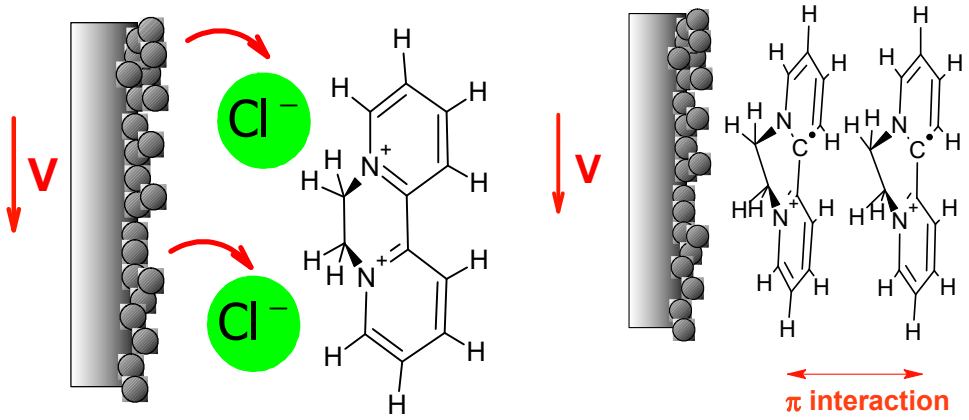

(**a**) (**b**)

Figure 5. Proposed mechanism of adsorption of DQ on metal electrode.

Finally, we would like to consider the participation of the CT mechanism in the SERS of DQ. Such a mechanism has been exhibited for the parent molecule 2,2′-bipyridine at about the same excitation wavelength [37] and the special characteristics of the adsorbed species of DQ that favor a stronger interaction between the metal and the ionic pair. As can be seen in Figures 2 and 3, the aromatic ring vibrational modes around 1580 cm^{-1} (key SERS-CT bands) are markedly higher in the SERS on the silver electrode at 785 nm when the electrode potential is more negative and at a lower wavelength than when the electrode potential is more positive. In the SERS on the copper electrode, this difference is not so outstanding, and there is similar behavior at both excitation wavelengths (Figure 2). The SERS enhancement behavior of DQ on the silver electrode is attributed to the manifested resonant Raman effect associated with the charge transfer of the diquat surface complex when using a lower excitation wavelength favored at positive electrode potentials. On the contrary, we need to use more negative potentials in order to obtain similar results when we record the SERS spectra at 785 nm. We plot the frontier molecular orbital HOMO and LUMO energy levels for the different species and metal complexes of DQ in Tables 1 and S1. The HOMO-LUMO energy gap is useful to evaluate the local and global chemical reactivity of the species and the electron-donating and the electron-accepting capabilities of the molecule. As shown in these results, the energy gap of the radical cation of DQ (2.62 eV) is similar to that of the metal complexes and the ionic pair metal complexes. In contrast, there are significant differences in the dication species DQ^{2+}. These results suggest that a CT process at a positive electrode potential could be conceivable from the metal to the molecule only if the radical cation species is adsorbed, forming the ionic pair.

4. Conclusions

We report here the first comparative SERS study of DQ on silver and copper electrodes, supported by DFT calculations. Our findings show that the DQ^{2+} species is very stable in solution, with no observable degradation over time into its reduction products, $DQ^{+\bullet}$ or DQ^{0}. The reduction process involves a decrease in the inter-ring angle as follows: DQ^{2+} (22.60°) > $DQ^{+\bullet}$ (14.31°) > DQ^{0} (4.76°). This increased molecular coplanarity in the reduced species accounts for significant differences in the Raman spectra of DQ. Notably, DQ exhibited different adsorption behaviors on the copper and silver electrodes. For potentials above −0.40 V, no sensitive differences were observed in the SERS of DQ on the two metals. However, when the potential reached −0.30 V, drastic changes were observed in the SERS spectra on the silver electrode at both excitation wavelengths.

An analysis of the SERS bands revealed that at more positive electrode potentials, the interaction of DQ with the metal forms a charge-transfer complex via the chloride anion adsorbed on the surface. At more negative potentials, other DQ species, distinct

from DQ^{2+}, form and adsorb on the surface. In addition, the resonance dependence of specific vibrational modes around 1580 cm^{-1} with the excitation wavelength implies that an SERS-CT mechanism is contributing to the SERS spectra of DQ. Finally, theoretical calculations of different DQ metal complexes suggest that the HOMO-LUMO energy gap is accessible for the excitation wavelengths employed if it is fulfilled that a positive electrode potential is applied. This also aligns with the presence of radical cation species adsorbed on the surface, forming the corresponding ionic pair.

Supplementary Materials: The following supporting information can be downloaded at: https://www.mdpi.com/article/10.3390/chemosensors13020039/s1, Table S1. DFT calculations of different metal complexes of DQ2+ at B3LYP/6-31+G* level of theory. Figure S1. Raman spectra of 1 M solution and solid state of DQ2+ recorded at different wavelengths: (a,b) 514.5 nm, (c,d) 632.8 nm and (e,f) 785 nm. Figure S2. SERS spectra of DQ2+ 10−3 M (a) and 10−5 M (b) on copper electrode recorded at 785 nm. Figure S3. SERS spectra of DQ2+ 10−5 M on silver electrode recorded at 514.5 nm.

Author Contributions: M.R.L.-R.: conceptualization; methodology; investigation; writing—original draft preparation; visualization; formal analysis; reviewing and editing. L.O.-F.: methodology; investigation; writing—original draft preparation; formal analysis. S.S.-C.: supervision, reviewing and editing. All authors have read and agreed to the published version of the manuscript.

Funding: This work was conducted with funding from the PID2023-146214OB-I00 project funded by MCIU/AEI/10.13039/501100011033 and FSE+. of the Spanish Ministry of Science and Innovation.

Institutional Review Board Statement: Not applicable.

Informed Consent Statement: Not applicable.

Data Availability Statement: The data presented in this study are available upon request from the corresponding author.

Acknowledgments: The authors thank the facilities of the laboratory of AFM and Raman Microscopy, at the SCAI (Central Services Research Support) of the University of Málaga (Spain) and Ra-fael Larrosa (the University of Málaga) for their computational facilities.

Conflicts of Interest: The authors declare no conflicts of interest.

References

1. Aroca, R. *Surface-Enhanced Vibrational Spectroscopy*; John Wiley & Sons, Ltd.: Hoboken, NJ, USA, 2006; ISBN 0-471-60731-2. [CrossRef]
2. Moskovits, M. Persistent misconceptions regarding SERS. *Phys. Chem. Chem. Phys.* **2013**, *15*, 5301. [CrossRef]
3. Pięta, E.; Paluszkiewicz, C.; Kwiatek, W.M.; López-Ramírez, M.R. Analyzing the Electrochemical Interaction of the Angiogenesis Inhibitor Batimastat by Surface-Enhanced Raman Spectroscopy. *Chemosensors* **2023**, *11*, 128. [CrossRef]
4. Pięta, E.; Lopez-Ramirez, M.R.; Paluszkiewicz, C.; Kwiatek, W.M. Insights into the binding interactions at the nano-bio interface: Electrode potential and wavelength dependence study. *Appl. Surf. Sci.* **2021**, *562*, 150228. [CrossRef]
5. Lopez-Ramirez, M.R.; Aranda Ruiz, D.; Avila Ferrer, F.J.; Centeno, S.P.; Arenas, J.F.; Otero, J.C.; Soto, J. Analysis of the Potential Dependent Surface-Enhanced Raman Scattering of p-Aminothiophenol on the Basis of MS-CASPT2 Calculations. *J. Phys. Chem. C* **2016**, *120*, 19322–19328. [CrossRef]
6. Roman-Perez, J.; Centeno, S.P.; López-Ramírez, M.R.; Arenas, J.F.; Soto, J.; López-Tocón, I.; Otero, J.C. On the dual character of charged metal–molecule hybrids and the opposite behaviour of the forward and reverse CT processes. *Phys. Chem. Chem. Phys.* **2014**, *16*, 22958–22961. [CrossRef] [PubMed]
7. Lopez-Ramirez, M.R.; Ruano, C.; Castro, J.L.; Arenas, J.F.; Soto, J.; Otero, J.C. Surface-Enhanced Raman Scattering of Benzoate Anion Adsorbed on Silver Nanoclusters: Evidence of the Transient Formation of the Radical Dianion. *J. Phys. Chem. C* **2010**, *114*, 7666–7672. [CrossRef]
8. Jones, G.M.; Vale, J.A. Mechanisms of Toxicity, Clinical Features, and Management of Diquat Poisoning: A Review. *J. Toxicol. Clin. Toxicol.* **2000**, *38*, 123–128. [CrossRef] [PubMed]
9. Vale, J.A.; Meredith, T.J.; Buckley, B.M. Paraquat poisoning: Clinical features and immediate general management. *Hum. Toxicol.* **1987**, *6*, 41–47. [CrossRef] [PubMed]
10. Bismuth, C.; Garnier, R.; Baud, F.J.; Muszynski, J.; Keyes, C. Paraquat Poisoning. *Drug Saf.* **1990**, *5*, 243–251. [CrossRef] [PubMed]

11. Monk, P.M.S. *The Viologens. Physicochemical Properties, Synthesis and Applications of the Salts of 4,4′-Bipyridine*; John Wiley & Son: Chichester, UK, 1999; ISBN 978-0-471-98603-4.
12. Haque, R.; Lilley, S. Infrared spectroscopic studies of charge transfer complexes of diquat and paraquat. *J. Agric. Food Chem* **1972**, *20*, 57–58. [CrossRef]
13. Barker, D.J.; Cooney, R.P.; Summers, L.A. Resonance Raman spectra of radical cations of bridged diquaternary salts of 2,2′-bipyridine. *J. Raman Spectrosc.* **1985**, *16*, 265–271. [CrossRef]
14. Lopez-Ramirez, M.R.; Guerrini, L.; Garcia-Ramos, J.V.; Sanchez-Cortes, S. Vibrational analysis of herbicide diquat: A normal Raman and SERS study on Ag nanoparticles. *Vib. Spectrosc.* **2008**, *48*, 58–64. [CrossRef]
15. Bird, C.L.; Kuhn, A.T. Electrochemistry of the viologens. *Chem. Soc. Rev.* **1981**, *10*, 49. [CrossRef]
16. Kreisig, S.; Tarazona, A.; Koglin, E. The adsorption of paraquat on silver electrode surfaces: A SERS microprobe study. *Electrochim. Acta* **1997**, *42*, 3335–3344. [CrossRef]
17. Li, S.; Ling, Y.; Chen, J.; Yuan, X.; Zhang, Z. Portable Copper-Based Electrochemical SERS Sensor for Point-of-Care Testing of Paraquat and Diquat by On-Site Electrostatic Preconcentration. *Langmuir* **2024**, *40*, 15677–15687. [CrossRef]
18. Rycenga, M.; Cobley, C.M.; Zeng, J.; Li, W.; Moran, C.H.; Zhang, Q.; Qin, D.; Xia, Y. Controlling the synthesis and assembly of silver nanostructures for plasmonic applications. *Chem. Rev.* **2011**, *111*, 3669–3712. [CrossRef]
19. Frisch, M.J.; Trucks, G.W.; Schlegel, H.B.; Scuseria, G.E.; Robb, M.A.; Cheeseman, J.R.; Scalmani, G.; Barone, V.; Mennucci, B.; Petersson, G.A.; et al. *Gaussian 09, Revision C.01*; Gaussian, Inc.: Wallingford, CT, USA, 2009.
20. Cojocaru, C.; Airinei, A.; Fifere, N. Molecular structure and modeling studies of azobenzene derivatives containing maleimide groups. *SpringerPlus* **2013**, *2*, 586. [CrossRef] [PubMed]
21. Spinner, E. The vibrational spectrum of the N-methylpentadeuteropyridinium ion. *Aust. J. Chem.* **1967**, *20*, 1805–1813. [CrossRef]
22. Pasquier, B.; Lebas, J.M. Contribution à l'étude vibrationnelle du biphényle. *J. Chim. Phys.* **1967**, *64*, 765–776. [CrossRef]
23. Forster, M.; Girling, R.B.; Hester, R.E. Infrared, Raman and resonance Raman investigations of methylviologen and its radical cation. *J. Raman Spectrosc.* **1982**, *12*, 36–48. [CrossRef]
24. Lu, T.H.; Sun, I.W. Determination of Diquat at a Nafion Film Modified Glassy Carbon Electrode Using Electrocatalytic Voltammetry. *Electroanalysis* **2000**, *12*, 605–609. [CrossRef]
25. Noh, H.B.; Chandra, P.; Moon, J.O.; Shim, Y.B. In vivo detection of glutathione disulfide and oxidative stress monitoring using a biosensor. *Biomaterials* **2012**, *33*, 2600–2607. [CrossRef]
26. Athira, K.; Ranjana, M.; Bharathi, M.S.S.; Narasimha Reddy, B.; Satheesh Babu, T.G.; Venugopal Rao, S.; Ravi Kumar, D.V. Aggregation induced, formaldehyde tailored nanowire like networks of Cu and their SERS activity. *Chem. Phys. Lett.* **2020**, *748*, 137390. [CrossRef]
27. Qiu, H.W.; Xu, S.C.; Chen, P.X.; Gao, S.S.; Li, Z.; Zhang, C.; Jiang, S.Z.; Liu, M.; Li, H.S.; Feng, D.J. A novel surface-enhanced Raman spectroscopy substrate based on hybrid structure of monolayer graphene and Cu nanoparticles for adenosine detection. *Appl. Surf. Sci.* **2015**, *332*, 614–619. [CrossRef]
28. Chen, H.Y.; Lin, M.H.; Wang, C.Y.; Chang, Y.M.; Gwo, S. Large-Scale Hot Spot Engineering for Quantitative SERS at the Single-Molecule Scale. *J. Am. Chem. Soc.* **2015**, *137*, 13698–13705. [CrossRef]
29. Kleinman, S.L.; Sharma, B.; Blaber, M.G.; Henry, A.I.; Valley, N.; Freeman, R.G.; Natan, M.J.; Schatz, G.C.; Van Duyne, R.P. Structure Enhancement Factor Relationships in Single Gold Nanoantennas by Surface-Enhanced Raman Excitation Spectroscopy. *J. Am. Chem. Soc.* **2012**, *135*, 301–308. [CrossRef] [PubMed]
30. Millán, J.I.; Ruiz, J.J.; Camacho, L.; Rodríguez-Amaro, R. Electroreduction of Heptyl Viologen on Polycrystalline Silver. *J. Electrochem. Soc.* **2002**, *149*, E440. [CrossRef]
31. Millán, J.I.; Garcia-Ramos, J.V.; Sanchez-Cortes, S.; Rodríguez-Amaro, R. Adsorption of lucigenin on Ag nanoparticles studied by surface-enhanced Raman spectroscopy: Effect of different anions on the intensification of Raman spectra. *J. Raman Spectrosc.* **2003**, *34*, 227–233. [CrossRef]
32. Lévi, G.; Pantigny, J.; Marsault, J.P.; Aubard, J. SER spectra of acridine and acridinium ions in colloidal silver sols. Electrolytes and PH effects. *J. Raman Spectrosc.* **1993**, *24*, 745–752. [CrossRef]
33. Oh, S.T.; Kim, K.; Kim, M.S. Adsorption and surface reaction of acridine in silver sol: Surface-enhanced Raman spectroscopic study. *J. Phys. Chem.* **1991**, *95*, 8844–8849. [CrossRef]
34. Monk, P.M.S.; Hodgkinson, N.M. Charge-transfer complexes of the viologens: Effects of complexation and the rate of electron transfer to methyl viologen. *Electrochim. Acta* **1998**, *43*, 245–255. [CrossRef]
35. Walcarius, A.; Lamberts, L. Square wave voltammetric determination of paraquat and diquat in aqueous solution. *J. Electroanal. Chem.* **1996**, *406*, 59–68. [CrossRef]

36. Heyrovský, M. The electroreduction of methyl viologen. *J. Chem. Soc. Chem. Commun.* **1987**, *24*, 1856–1857. [CrossRef]
37. Srnová-Šloufová, I.; Vlčková, B.; Snoeck, T.L.; Stufkens, D.J.; Matějka, P. Surface-Enhanced Raman Scattering and Surface-Enhanced Resonance Raman Scattering Excitation Profiles of Ag-2,2′-Bipyridine Surface Complexes and of $[Ru(bpy)_3]^{2+}$ on Ag Colloidal Surfaces: Manifestations of the Charge-Transfer Resonance Contributions to the Overall Surface Enhancement of Raman Scattering. *Inorg. Chem.* **2000**, *39*, 3551–3559. [CrossRef]

Disclaimer/Publisher's Note: The statements, opinions and data contained in all publications are solely those of the individual author(s) and contributor(s) and not of MDPI and/or the editor(s). MDPI and/or the editor(s) disclaim responsibility for any injury to people or property resulting from any ideas, methods, instructions or products referred to in the content.